Study of the Heat-Assisted Milling of Ti–6Al–4V Under Dry and Minimum-Quantity-Lubrication

Şener Karabulut[1] · Musa Bilgin[1] · Halil Karakoç[1] · Dimitrios Skondras Giousios[2] · Angelos P. Markopoulos[2]

Abstract

In the present study, a pre-heating process was employed on Ti–6Al–4V alloy to overcome the machining difficulties in milling and the influence of the pre-heating on surface roughness, vibration, power consumption, and cutting tool wear was investigated. The experiments were conducted based on a Taguchi L18 orthogonal array at room temperature, hot, and hybrid cutting environments. A finite element analysis (FEM) was used to predict the temperature field on the surface of the workpiece during the hot machining of the Ti–6Al–4V alloy. The optical evaluation and microhardness measurements were carried out to determine the effect of the open flame preheating process on the machined surface and subsurface. The results revealed that a reduction of 106% and 64% in vibration and power consumption was achieved in the hybrid milling compared to dry milling, respectively. The mean tool wear was measured as 0.06 mm in the hybrid milling whereas the mean tool wear was 0.35 mm in the dry milling. Surface roughness was slightly worsened by a 15% rate due to the adhered materials particles on the machined surface in the hot and hybrid milling. The grain sizes and microhardness on the machined surfaces were not negatively affected by the pre-heating process.

Keywords Ti–6Al–4V · Tool wear · Hot milling · Surface roughness · Power consumption · Vibration

1 Introduction

Titanium and titanium alloys have high fracture toughness, fatigue, creep resistance, corrosion resistance, and biocompatibility with a high strength to weight ratio. Due to these physical and mechanical properties, titanium alloys are highly preferred in various engineering applications in aviation, marine, chemistry, and medical industries [1, 2]. Despite these superior physical and mechanical properties, the low thermal conductivity of titanium, strain hardening, low elastic modulus, and chemical affinity with the cutting tool at high temperatures during machining lead to rapid tool failures [3]. Since the processing of titanium alloys with conventional techniques is very difficult and costly, engineers have performed research on the machinability of titanium and its alloys using different cutting environments such as cryogenic cooling [4, 5], heating [6, 7], lubrication, and hybrid techniques [1, 8].

Hot machining studies have become increasingly popular under different heating technics recently [6] due to the effective machining problems of titanium alloys which are classified as difficult to cut materials with traditional methods. In hot machining, the work material is thermally softened and its shear strength is reduced. Thermal softening of the workpiece contributes to a reduction in cutting resistance and thus reduces the cutting force [9]; vibrations and improves the tool life [10]; and surface roughness [11]. Conventional machining methods on processing materials can lead to lower surface quality and shorten tool life. Heat-assisted machining (HAM) is generally an effective and sustainable method to solve such problems. When processing the workpiece at elevated temperatures softening is caused which is expected to improve machinability [12]. Different methods have been proposed on how the heat assisting is implemented during the manufacturing procedure as well as how these different approaches affect machining parameters like surface roughness, cutting conditions and tool life. Plasma-assisted machining (PAM) pertains to the use of

✉ Şener Karabulut
  senerkarabulut@hacettepe.edu.tr

[1] Department of Mechanical Program, Hacettepe University, 06930 Ankara, Turkey

[2] School of Mechanical Engineering, National Technical University of Athens, 15780 Athens, Greece

a plasma jet heat source along with conventional machining (CM). Although it is not widely researched recently, PAM is known to improve material removal rate (MRR) [13] as well as cause a decrease of cutting forces and surface roughness [14, 15]. However, it is not cost effective and can cause material degradation [16]. Another approach of HAM is laser-assisted machining (LAM) which involves a laser source for preheating the material surface before machining. LAM has been used in milling, among other processes. Compared with CM it is considered beneficial for optimizing machining parameters e.g., surface roughness [17] cutting forces and tool wear [18, 19] of difficult-to-cut metals and ceramics. However, using a laser source can be associated with high cost. HAM can be also employed by induction heating, usually with an induction coil as heating source. Induction pre-heating in milling hard-to-cut materials is reported to improve chatter effects [20], tool life [21], cutting forces, and surface roughness. However, it can cause changes to microstructure [10] and can lead to tool failure due to thermal effects, when using uncoated tools [22]. Compared to LAM, induction-assisted machining (IAM) is considered more cost-effective, although LAM can lead to better machinability [22, 23]. The use of flame for assisting machining processes is also frequently used due to cost-effectiveness. Regarding turning processes in materials of high-strength like titanium or nickel-based alloys, it has been found that flame assistance leads to improved tool life [11, 24], reduction of surface roughness and cutting forces [11, 25, 26], reduction of flow stress [27], and chip thickness [28]. An enhancement of microhardness and no phase changes in flame-assisted machining of Inconel 718 were additionally observed [25]. Regarding milling of stainless steel, a decrease of cutting forces, had a beneficial effect on surface quality and tool life, even with uncoated inserts [29]. Other types of thermal assisted and hybrid methods that lead to improved machinability have been utilized, including furnace preheating [30], combination of different heat sources [9], electrical discharge assistance [31] and ultrasonic peening [32].

Considering the above-mentioned literature review a lot of studies are available on the machining of difficult-to-cut materials such as Ti–6Al–4V, stainless steel and Inconel 718 [33]. The researchers have reported the advantages of the MQL in the machining of titanium alloys [34, 35] and mentioned the benefits of hot machining above. The literature review indicated that MQL-assisted hot milling has not been studied before. Therefore, the presented study aimed to combine the advantages of the MQL in terms of cooling and lubrication effects on the cutting insert and the thermal softening influence of heat-assisted machining on the workpiece. For this reason, the MQL was applied to the cutting tool's rake surface to utilize the cooling and lubrication effects during the milling of preheated Ti–6Al–4V. Then, the influences of dry milling at room temperature, hot and MQL-assisted

hot machining (hybrid) were investigated compared with the surface roughness, vibration, power consumption, and tool wear. The microstructural evolutions of the machined surface were assessed by optical microscope observations and microhardness measurements to determine the effect of the hot machining process on the grain size of the machined surface. Additionally, experimental results were analyzed by the means of the analysis of variance and mean effect graphs and the results of dry, hot, and hybrid machining were compared.

2 Materials and Methods

2.1 Experimental Procedure

A set of machining experiments were performed in order to evaluate the influence of hot and hybrid cutting environment on the milling behavior of the Ti–6Al–4V titanium alloy. The chemical compositions and the hardness of Ti–6Al–4V titanium alloy delivered by the supplier are presented in Table 1. The milling experiments of titanium alloy were conducted on a Frontier MCV-866 CNC vertical machine tool. Two Mitsubishi SOMT12T308PEER-JM VP15TF grade PVD coated carbide cutting inserts at an entering angle of 90° were used with a standard BT 40 tool holder for the tests, and each cutting process was carried out using a new edge. The workpiece material machined in the present study was supplied as a forged alpha–beta microstructure titanium of 300 mm × 196 mm × 50 mm dimensions. Then, the workpiece was cut into three equal parts with dimensions of 196 mm × 96 mm × 50 mm using the wire electrical discharge machining (Wire EDM) to minimize the variability in material properties.

The up-milling strategy by performing straight-face milling operations along 196 mm was used during the experiments due to the chip thickness starting at zero and increasing toward the end of the cut. In order to verify the experimental results, the machining tests were repeated twice and calculated the average values of the measured values of both experiments. Four milling variables, namely, cutting environment, feed rate and cutting speed each at three levels and axial depth of cut at two levels were chosen based on the Taguchi L18 orthogonal array design of experiments (DoE). During the experiments, machine vibration, vibration acceleration, and power consumptions were recorded instantly, tool wear and surface roughness were selected as decisive criteria for the experimental study.

The milling tests were done under three different cutting environments, dry at room temperature, hot machining, and hybrid machining. The cutting speed and feed rates values used in the tests were determined in accordance with the preliminary experiment results. The preliminary milling experiments were conducted according to the catalogue data for the cutting tool and ISO Standard 8688-1 [36]. A

Table 1 Chemical composition of Ti–6Al–4V alloy

Al (%)	V (%)	C (%)	Fe (%)	O (%)	N (%)	H (%)	Hardness
5.5–6.5	3.5–4.5	0.08	0.25	0.2	0.05	0.0015	335 HV

biodegradable cutting oil, namely Viscol Viscut (Kinematic viscosity at 40 °C: 37–40 cSt, density at 15 °C: 0.88 g/cm^3, flash point > 240 °C) was used with a WERTE STN40 lubrication system at the hybrid milling environment of Ti6Al4V. The cutting oil was directly applied to the deformation zone for effective lubrication and air cooling at the cutting interface. The MQL nozzle was focused onto the insert nose 15 mm away from the cutting point with a 20° angle to the machine's XY plane and the flow rate of the oil was adjusted to 10 ml/min.

2.2 Milling Environments

To compare the effect of pre-heating to the titanium alloy on machined surface quality, cutting tool wear, vibration, and energy consumption for this study, three different cutting environments were used in the experiments: dry, hot machining, and hybrid-hot machining with MQL. The hybrid hot machining with MQL will be mentioned as hybrid machining from this point.

(i) *Dry-machining at room temperature:* Milling tests were conducted at room temperature under dry environments. The workpieces used in this experiment were not subjected to heating. The dry milling environment was identified as a check parameter for this experimental study.

(ii) *Hot machining*: Since the preheating of the workpiece decreases the shear strength and supports easier chip removal. The workpiece material was preheated to 250 °C by an external heat source for 10 min using the open flame method. The workpiece surface temperature was monitored with the MI3 pyrometer during the heating process of the workpiece. When the surface temperature reached 250 °C, the external heat source was stopped and the cutting process was put to start under a dry machining environment.

(iii) *Hybrid-machining*: In this machining environment, the external heating was stopped after the workpiece surface temperature was heated up to 250 °C and MQL was applied to the cutting point during the milling process. The heated workpiece was lubricated with pressurized air directly to the cutting area to diminish the friction in the tool/chip interface at the tool's rake face and between the workpiece and flank side of the tool. For this purpose, the MQL nozzle is positioned to focus on the cutting point in order to provide effective cooling and lubrication on the insert with compressed air.

2.3 Experimental Measurements and Microstructural Evaluations

A Mitutoyo SJ-210 was utilized to determine the machined surface quality. Five separate points on the surface of the workpiece were measured, and the average surface roughness values were determined by eliminating unsuitable values. The surface temperature of the workpiece was continually monitored and recorded utilizing a Raytek infrared pyrometer during the experiments. The measured data were conveyed to the computer via a USB cable and logged in an Excel file. CNC milling machine was equipped with a Fluke 43B series power-quality analyzer to measure energy consumption during the experiments. The machine vibration and vibration acceleration generated by the machining parameters were measured using a banner QM42VT2 vibration measurement sensor. The device was mounted on the vice and connected to politrace smart box and the data were stored on the politrace web page. Tool wear measurements were made using a Zoller Venturion device with "lasso" software which can easily capture the tool contour and worn areas on the tool. The wear mechanism of cutting inserts was examined using a TESCAN MAIA3 XMU Scanning electron microscopy (SEM) and an optical microscope. In order to evaluate the influence of three different machining conditions on the surface hardness of the workpiece, a DuraScan-G5 microhardness measurement device was used with the application of a testing force of 2.942 N for a period of 10 s (EN ISO 6507-1) along the centerline of the machined surface, moving with steps of 1 mm.

2.4 Experimental Design

In this study, optimal milling parameters and their effects on tool wear, power consumption, vibration, and surface roughness are investigated in the milling of titanium alloy under different cutting environments. Taguchi L18 ($2^1 \times 3^3$) DoE is employed to reduce experimental process and cost which requires a total of 54 experiments with full factorial experimental processing parameters, thus the effects of uncontrolled factors are minimized. Taguchi's loss-of-quality function approach is used to compute the deviation between optimum processing values and experimental

Table 2 Milling variables and levels

Factors	Notation	Units	Level 1	Level 2	Level 3
A, Cutting environments	C_e	–	Dry	Heat	Heat + MQL
B, Cutting speed	V_c	m/min	40	60	75
C, Feed rate	f_z	mm/tooth	0.15	0.20	0.25
D, Axial depth of cut	a_p	mm	1	1.5	–
Radial depth of cut	a_e	mm	30		
Diameter of tool holder	D_c	mm	63		
Number of cutting insert	Z_c	Piece	2		
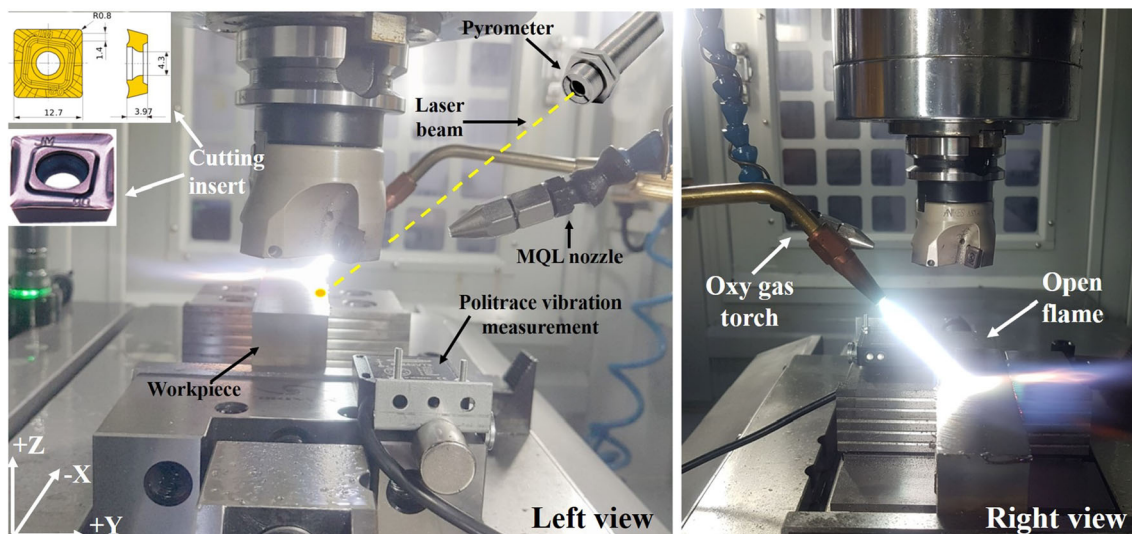
Fig. 1 Overview of heat-assisted milling test setup

results. This function converts output data into signal-to-noise (S/N) ratio, analyzes processing parameters according to S/N and evaluates measured values to target data under different noise conditions. For static designs, one of the three different *S/N* ratios can be chosen depending on the aim of the study: smaller is better, larger is better, and nominal is best. This work aims to optimize cutting tool wear, power consumption, surface roughness, and vibration. Therefore, a "smaller is better" ratio has been chosen to define the smallest values of the output parameters since it generates higher S/N ratios and best describes the state of the surface roughness, power consumption, cutting tool wear, and vibration.

$$S/N = -10 \times \log_{10}\left(\sum \frac{y^2}{n} y\right) \quad (1)$$

where *y* is the recorded output data for the vibration, power consumption, tool wear, and surface roughness.

Three levels were settled for the control factors of cutting environment, cutting speed, and feed rate, and axial depth of cut was adopted as two-levels. The test variables and design layout are presented in Table 2 (Figs. 1, 2).

3 Experimental Results and Discussion

In the present study, Ti–6Al–4V was machined with 18 milling experiments according to the Taguchi DoE, and six confirmation tests were conducted to verify the experimental results. The mean tool wear, surface roughness, vibration, and power consumption values and their corresponding S/N ratios are presented in Figs. 3, 4, 5, 6.

The experimental results were evaluated by using Minitab software to examine the influence of heating and hybrid milling on surface roughness (*Ra*), power consumption (*P*), machine tool vibration (*V*), and tool wear (*VB*). The micro-hardness measurement and microstructural evaluation were performed to clearly analyze the effects of the pre-heating on the machined surface and subsurface of the workpiece.

### 3.1 Surface Quality, Vibration, Power Consumption, and Tool Wear

The SEM images of machined surfaces under dry, hot and hybrid cutting environments were presented in Fig. 2a–c. Figure 2d belongs the machined surface SEM image obtained
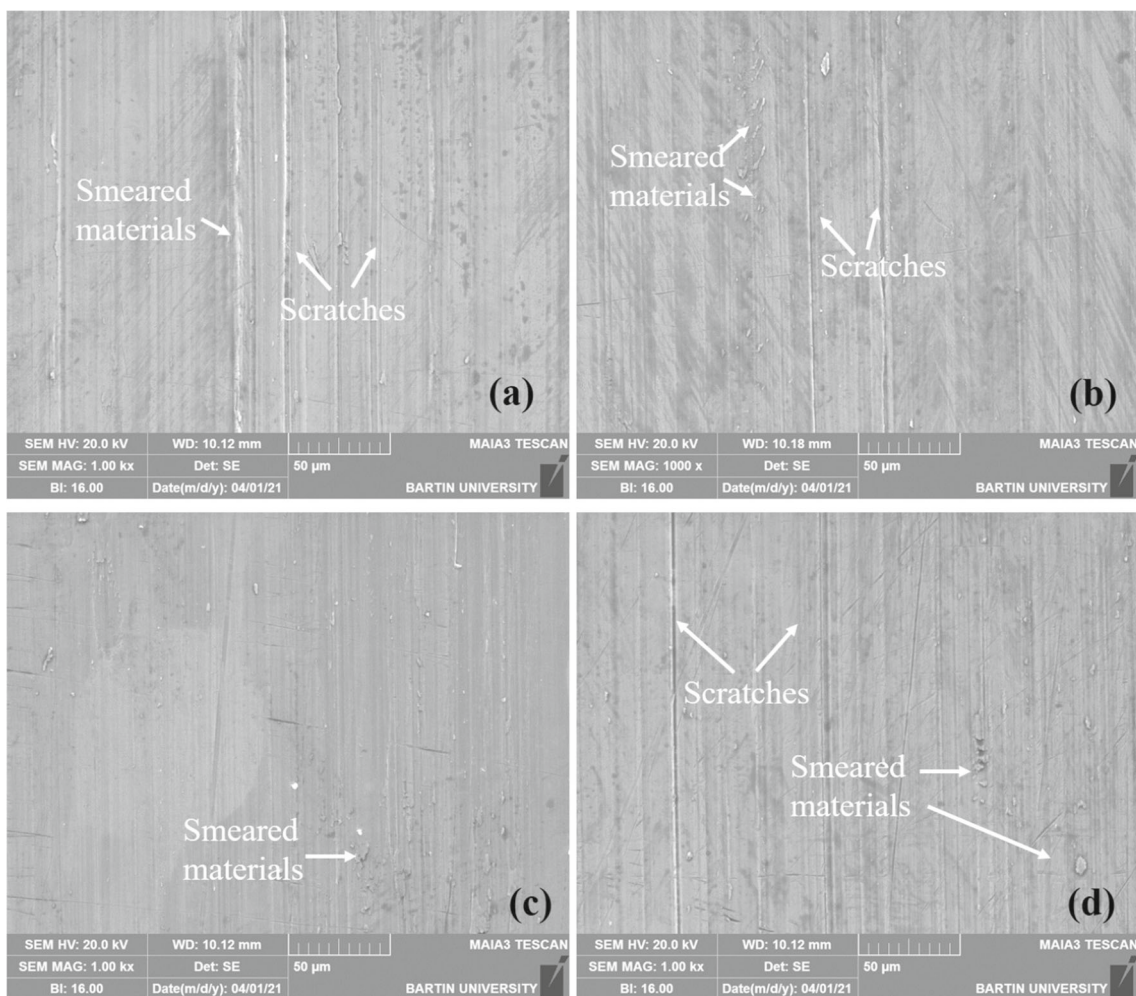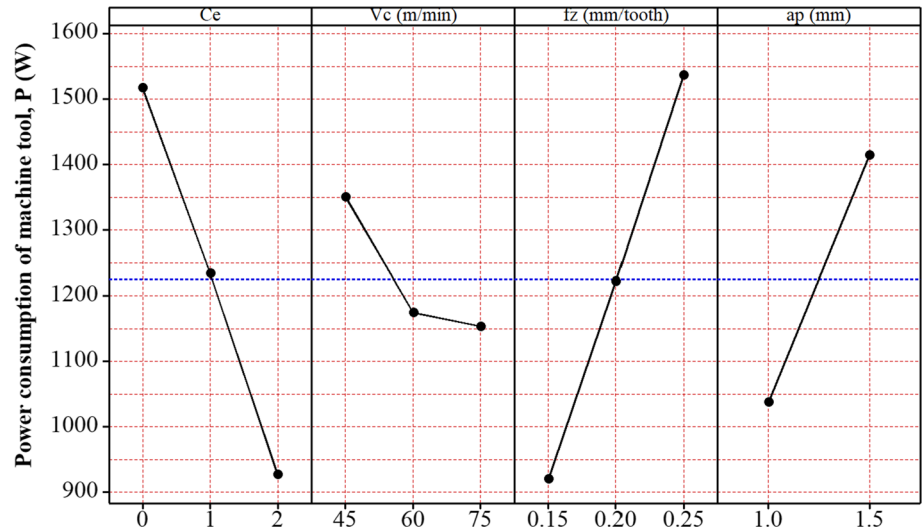
Fig. 2 SEM images of machined surfaces **a** Dry milling ($V_c = 75$ m/min, $f_z = 0.25$ mm/tooth, $a_p = 1$ mm), **b** hot milling ($V_c = 75$ m/min, $f_z = 0.25$ mm/tooth, $a_p = 1$ mm), **c** hybrid milling ($V_c = 60$ m/min, $f_z = 0.20$ mm/tooth, $a_p = 1.5$ mm) and **d** hybrid milling ($V_c = 75$ m/min, $f_z = 0.20$ mm/tooth, $a_p = 1$ mm)
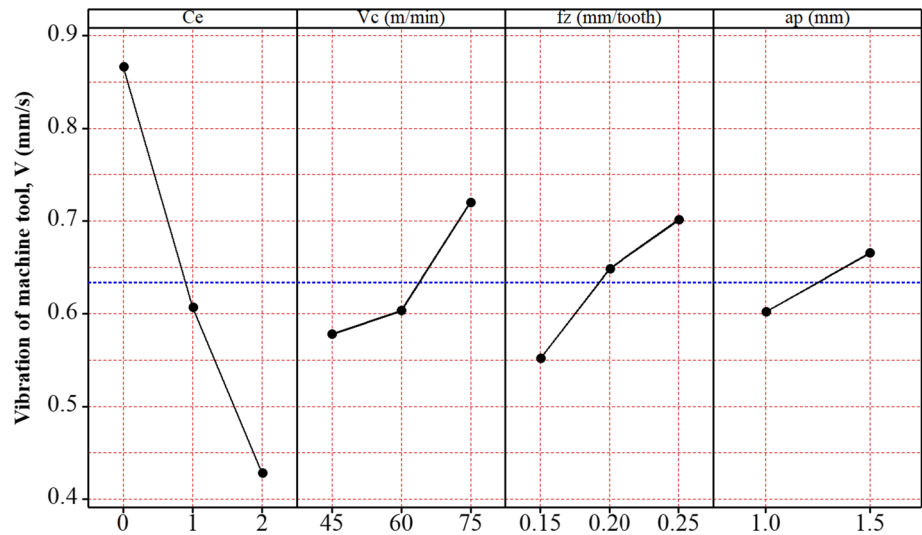

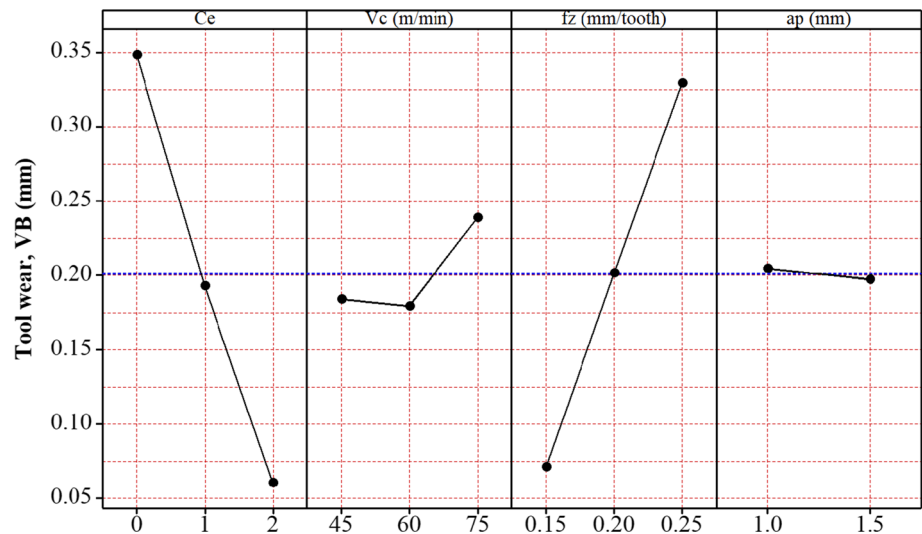**Fig. 3** Mean effects of cutting variables on surface roughness
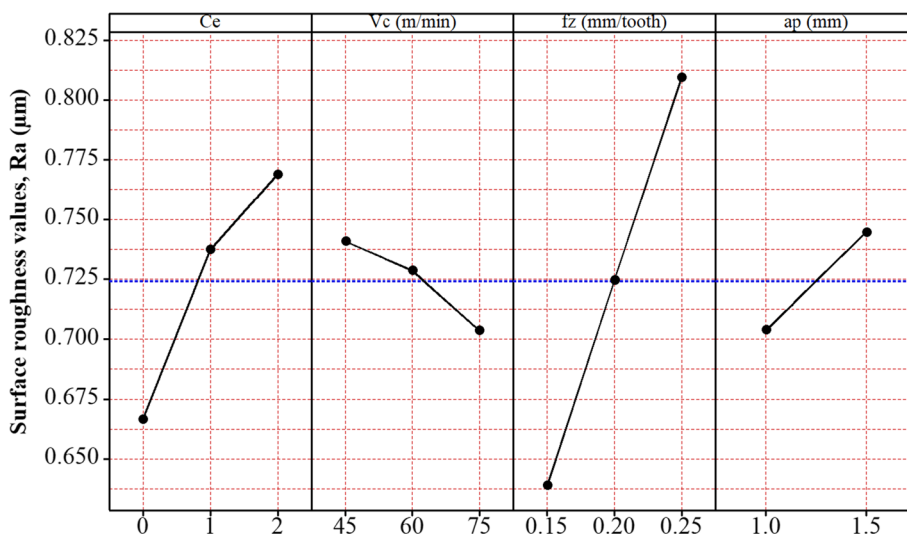
Fig. 4 Mean effects of cutting variables on power consumption

Fig. 5 Mean effects of cutting variables on machine tool vibration

Fig. 6 Mean effects of cutting parameters on tool wear values

from confirmation experiments conducted by under hybrid cutting environment. The surface roughness measurements were conducted at five different zones after cooled the workpiece for all milling experiments.

The unsuitable measurements were excluded and the average values were derived and depicted in Fig. 3. Lower surface roughness values were measured under dry milling environment at room temperature. The surface quality deteriorated with increasing cutting feed and axial depth of cut in all milling parameters and improved at a higher cutting speed, as expected. Hence, it can be stated that the surface quality of the machined workpiece was not significantly affected by the milling environments used in the experiments. It can be expected an enhancement in the quality of the workpiece due to the reduction of friction and easier cutting process under hot and hybrid cutting conditions. In addition, it is known to reduce surface roughness in general, as lubrication reduces frictional forces during machining. However, in this study, the titanium alloy exhibited a ductile behavior due to the preheating process and caused the adhesion of a small amount of material on the machined surface (Fig. 2). Therefore, surface roughness values slightly increased due to the smeared materials on the machined surface whereas the machine vibration and power consumption decreased under a hot machining environment [21]. Similar surface defects were reported by Sarıkaya et al. [35] in machining of Ti–6Al–4V.

The mean effect graph shows that the surface roughness values decreased from 0.75 to 0.70 μm with increasing cutting speed. Hence, it can be said that the cutting speed had a very limited influence on surface roughness, power consumption, and vibration compared to other parameters. Meanwhile, surface roughness values raised from 0.64 to 0.80 μm with rising cutting feed values in all machining environments. Higher cutting feeds cause higher friction between the cutting insert and part. Therefore, tool wear, power consumption, vibration, and surface roughness increased at higher cutting feeds (Figs. 3, 4 and 5).

The axial depth of cut did not present a significant influence on the surface quality of the workpiece and surface roughness values increased from 0.70 to 0.74 μm at higher cutting depth. It was seen that higher cutting depth was not affected the vibration values however it has a negative effect on the power consumption. Although hot and hybrid machining has a little negative impact on workpiece surface quality, it was observed that the vibration and power consumption significantly reduced compared to under dry cutting conditions at room temperature. The highest power consumption and vibration values were noted in milling at room temperature environment as 1517 W and 0.866 m/s, respectively.

The average power consumption and vibration values under hot cutting environment were 1233 W and 0.606 m/s, respectively. Therefore, power consumption and vibration values decreased by 19% and 30%, respectively. Pre-heating

of the workpiece prior to machining and continuing heating during the cutting process caused thermal softening of the titanium alloy and reduced its shear strength. The reduction in power consumption and the acceleration amplitude of the vibration shows that the cutting strength of the workpiece material was reduced and an easier cutting operation was conducted. The lowest average power consumption and vibration values were 927 W and 0.42 m/s and resulted in an improvement of 39% and 52%, respectively under hybrid machining conditions. The hybrid machining system was outperformed according to milling at room temperature and hot milling environments because the high-pressure air containing oil droplets in the MQL system supported to decrease the friction surface between the workpiece and cutting insert. The shear plane angle increased with the decreasing tool-chip workpiece interface friction and reduced chip thickness. Hence, the reduced primary deformation zone and shear plane area diminished the energy required for material removal [37] and also indicated a positive effect on tool wear. It was observed that the findings of MQL supported hybrid milling experiments were found to be consistent with studies in the literature [34, 38, 39]. The effects of milling parameters on tool wear are shown in Fig. 6 with the mean effect graph. It can be seen that the cutting environment and feed rate were the two main factors affecting tool wear. The highest tool wear of 0.62 mm was measured in the dry milling environment, and the lowest tool wear of 0.003 mm was obtained in the hybrid milling environment. It was observed that the tool wear values increased with increasing feed values whereas the cutting speed and depth of cut were not exhibited a meaningful effect on the tool wear.

3.2 Estimation of Thermal Effects by the Flame Torch on the Workpiece

As it was shown in the previous subsections, the influence of workpiece preheating by the flame was evident in various aspects of the milling process such as the power consumption, vibrations and tool wear. However, due to the fact that temperature was not directly measured, the influence of the additional heat input to the workpiece cannot be quantified and its variation in respect to process conditions is not directly investigated. For that reason, a FEM thermal model which predicts the temperature field in the workpiece due to the heat contribution from the flame was developed.

In this model, both steps of the experimental procedure are simulated, namely the initial pre-heating and the heating of the workpiece after the process has begun. At the first step, the heat source remains at a constant position at the one end of the workpiece for 10 min (600 s) until a temperature of 250 °C (523 K) is reached, exactly at the point where the flame is focused, where the temperature was measured using the infrared pyrometer. The flame is modeled as
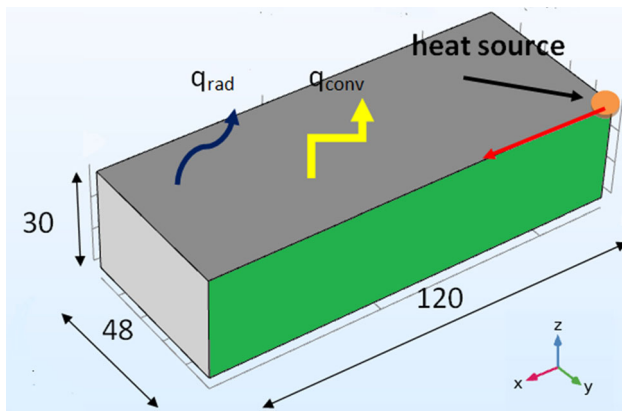
Fig. 7 Schematic of the FEM thermal model

a heat source whose flux is considered to be approximated by a gaussian distribution with a diameter of 3 mm, which corresponds directly to the diameter of the actual nozzle for the flame torch. Due to the fact that there is no generally accepted model for modeling the heat flux of a flame torch, an appropriate inverse approach is adopted in which the heat flux is determined after conducting simulations with different values until the conditions measured at the end of the first step of the heating process are met. As the model is thermal, the cutting procedure is not simulated and thus the prediction of the temperature field due to the action of the cutting tool in the workpiece is not performed. However, this model is very useful, as it can show the effect of pre-heating in the regions of the workpiece which the cutting tool will reach in a short time and can help to understand the extend of the beneficial effects of the flame torch due to the softening of workpiece material. So, in the second step of the simulation, the heat source moves at a velocity equal to the feed speed of the workpiece until it reaches the other end of the workpiece.

The simulation of both steps is carried out for three different conditions, namely the experimental conditions 4–6 for which the feed and cutting speed values are (0.15 mm/rev, 45 m/min), (0.20 mm/rev, 60 m/min) and (0.25 mm/rev, 75 m/min) respectively. A box-shaped workpiece is used in the simulation model, with dimensions of $120 \times 48 \times 30$ mm, which are a bit shorter in the feed and height direction. These choices are justified, as it was observed from preliminary simulations that the main amount of heat produced by the flame torch does not penetrate deeper than 30 mm in the workpiece and in the feed direction the temperature is almost stabilized after a few tens of millimeters. For the same reason the remaining surfaces were considered insulated, avoiding extra computational cost. As can be seen in Fig. 7, in the middle plane along the y-axis, denoted by green color, symmetry boundary conditions are imposed in order to take into account the exact width of the experimental workpiece but simulate half of the workpiece. Initial temperature is 293 K

(27 °C). On the top surface, convection and radiation boundary conditions are imposed. An appropriate mesh consisting about 18,000 3D hexahedral finite elements was created. An appropriate mesh with finer elements near the symmetry plane and coarser elements away from this plane is used in order to for the model to be able to simulate the heating process accurately but do not require an excessive amount of computational time. In the areas with smaller elements, their dimensions are smaller than the diameter of the flame torch in order to be able to take into account its heat flux appropriately. The average time of simulations was between 12 and 13 h and were carried out using an Intel Core i7 processor of 2.3 GHz with a 16 GB 1600 MHz DDR3 RAM.

After the simulations were carried out, the results were analyzed to determine the effect of heat assistance to the milling process. For the first step of the simulation, namely the initial pre-heating stage, it is worth observing the gradual penetration of heat in the workpiece. Thus, temperature isosurfaces are plotted in Fig. 8 at three different timesteps. From these figures, it can be seen that at the end of the first step, heat has penetrated considerably from the side of the workpiece and the temperature has risen over 293 K for several millimeters for its edge.

During the second stage, when the heat source moves before the cutting tool, a considerable amount of heat is introduced to the workpiece but it depends also on the feed speed. In Fig. 9 the temperature field is plotted at a section of the workpiece along the middle line at three different timesteps for the case of experiment in Fig. 10d. Moreover, the temperature profile along the middle line is plotted for each timestep as well. It can be seen that in every case, the temperature is relatively lower than the initial pre-heating stage temperature as it was expected, and that the heat source affects a small region in its vicinity, whereas its influence diminishes at larger distances and any unfavorable thermal effects are avoided in regions of the workpiece which will not be removed by the subsequent action of the cutting tool.

The average temperature for the three simulations during the second stage was 222.8 °C, 209.6 °C and 200.3 °C respectively. From these results, it becomes evident that generally, the increase of feed speed leads to a lower increase of temperatures due to the heat source, and the temperature drop from the initial pre-heating temperature for each simulation is 27.2 °C, 40.4 °C and 49.7 °C in each case. Thus, although in the case of the lower feed and cutting speed the temperature is closer to the initial one, in the case of the moderate and high feed speed a noticeable difference is observed. Consequently, it is suggested that in order to obtain the desired assistance from the heat source it is necessary to use lower feed speeds.
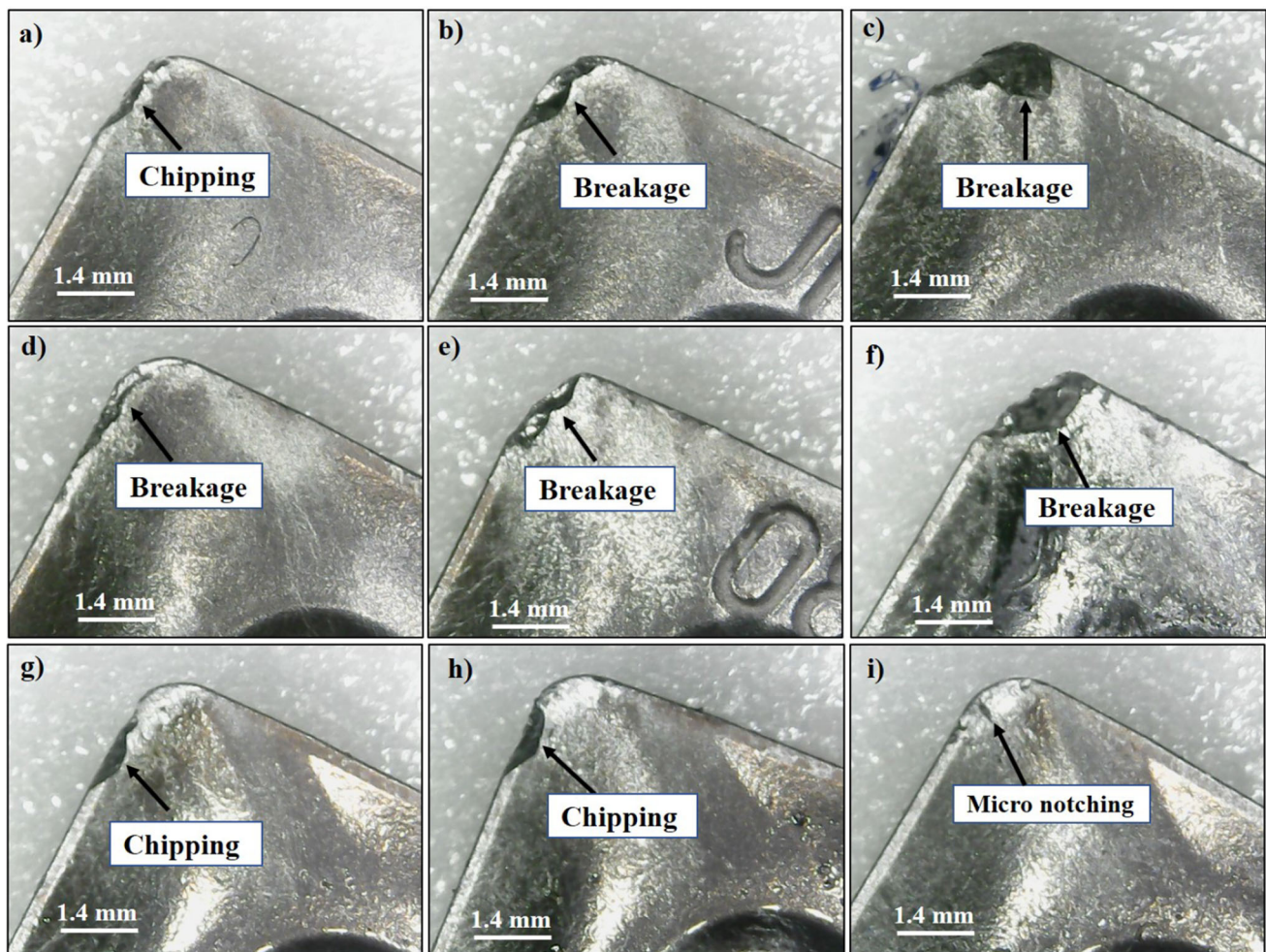
These observations are consistent with the experimental findings, presented in Figs. 3, 4, 5, 6 and can justify the results obtained in the cases where a heat source was employed.

Fig. 8 Temperature isosurfaces at three different timesteps during the initial pre-heating stage
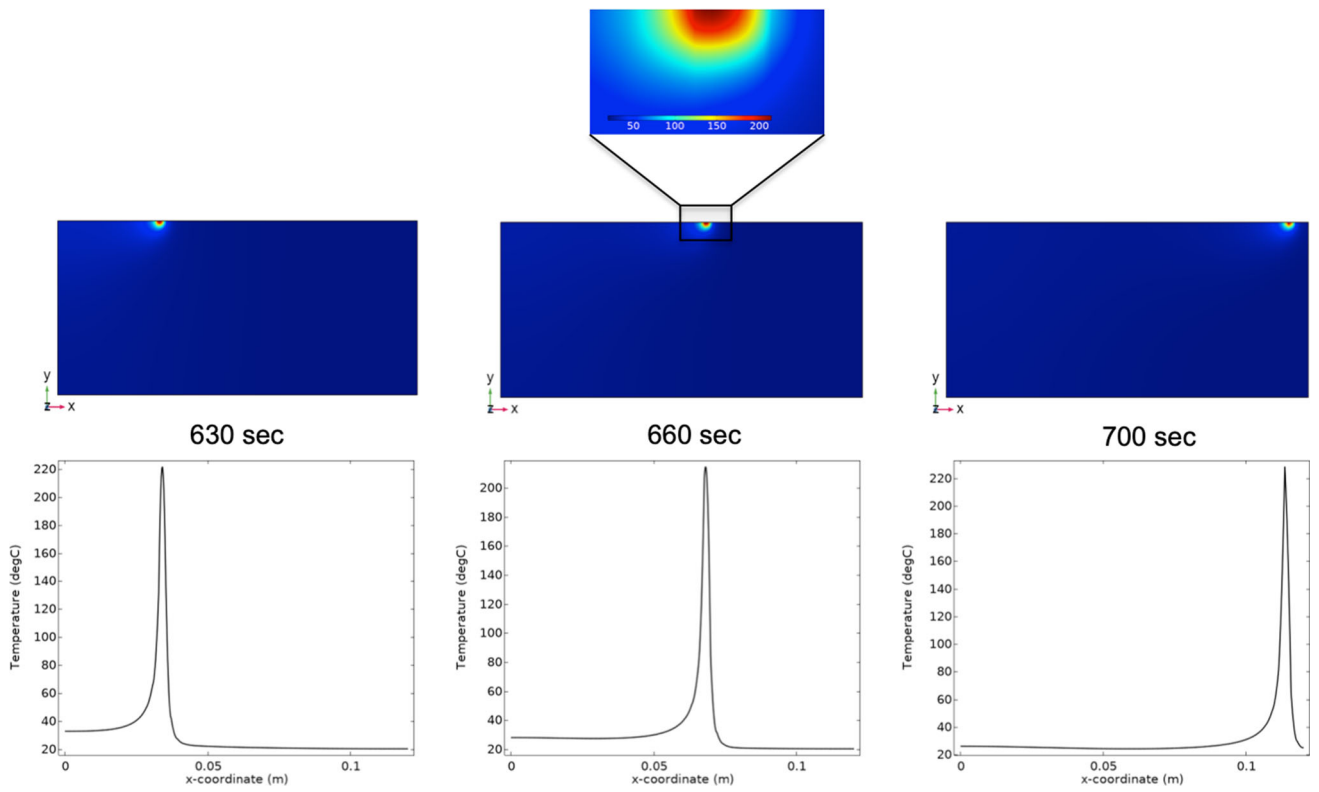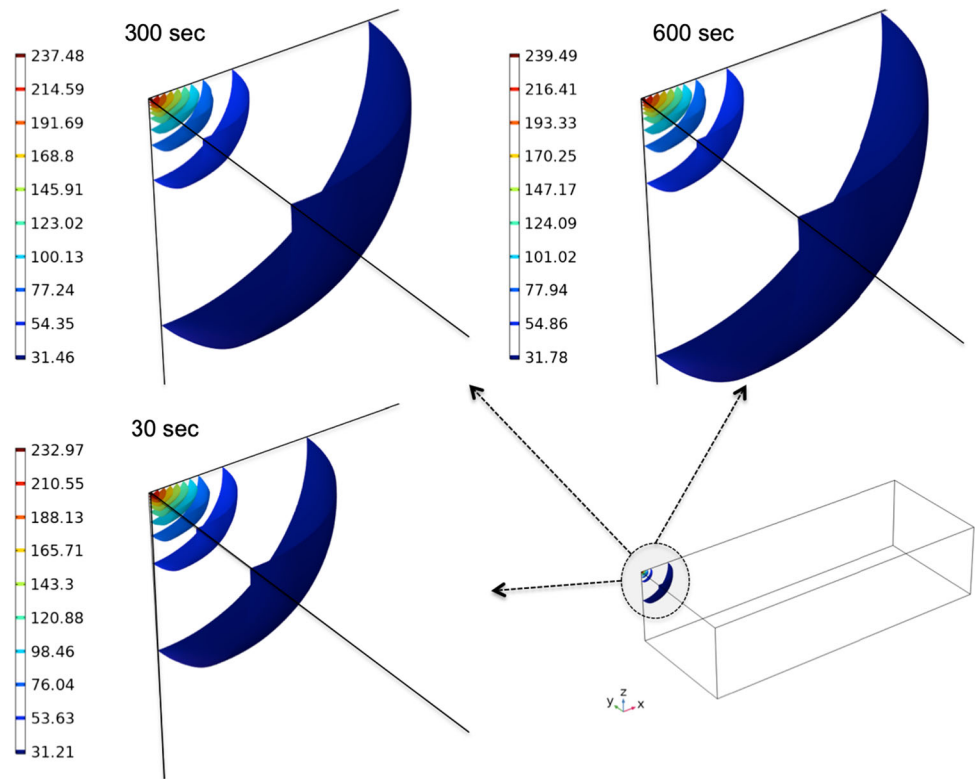
Fig. 9 Temperature field on the middle plane at different timesteps

Fig. 10 Microscopic wear images of the cutting tool's rake surface (a_p = 1 mm), **Dry milling**: **a** $V_c = 45$ m/min, $f_z = 0.15$ mm/tooth, **b** $V_c = 60$ m/min, $f_z = 0.20$ mm/tooth **c** $V_c = 75$ m/min, $f_z = 0.25$ mm/tooth, **Hot milling:** **d** $V_c = 45$ m/min, $f_z = 0.15$ mm/tooth, **e** $V_c = 60$ m/min, $f_z = 0.20$ mm/tooth, **f** $V_c = 75$ m/min, $f_z = 0.25$ mm/tooth, **Hybrid milling:** **g** $V_c = 45$ m/min, $f_z = 0.20$ mm/tooth, **h** $V_c = 60$ m/min, $f_z = 0.25$ mm/tooth, **i** $V_c = 75$ m/min, $f_z = 0.15$ mm/tooth

From the findings of these Figures, it can be observed that a considerable decrease in power consumption, vibrations and tool wear is obtained during hot machining in comparison with dry machining which was a result of the material softening caused by the increased temperature of the cutting area. FEM model results proved the experimental results. However, the beneficial effects of hot machining are more obvious in cases with lower feed and cutting speed, especially for tool wear. This can be directly attributed to the increased temperature due to the heat source, which affects the material properties directly in front of the cutting tool. The cutting tool is experiencing lower resistance from the workpiece material and thus, power consumption is reduced due to lower cutting forces, more stable cutting was achieved due to lower vibrations and also the progression of tool wear is affected, leading to a considerable reduction of VB in the case of the lower feed and cutting speed values when the highest temperature due to the heat source is observed.

3.3 Analysis of Cutting Tool Wear

The cutting insert failures on the rake face of used tools in the experiments are depicted in Figs. 10 and 11, respectively. The cutting tool performance is a key parameter in determining the machinability behavior of engineering materials, and different wear mechanisms occur depending on the material being machined. Tool wear is a failure mechanism of the cutting tool preventing optimal material removal during the cutting process. Therefore, it is important to define and reduce the tool wear during normal tool life. Tool wear rates can be seen from the images of the optical microscope in milling of titanium alloy under different cutting conditions. The heat produced during the milling of titanium is
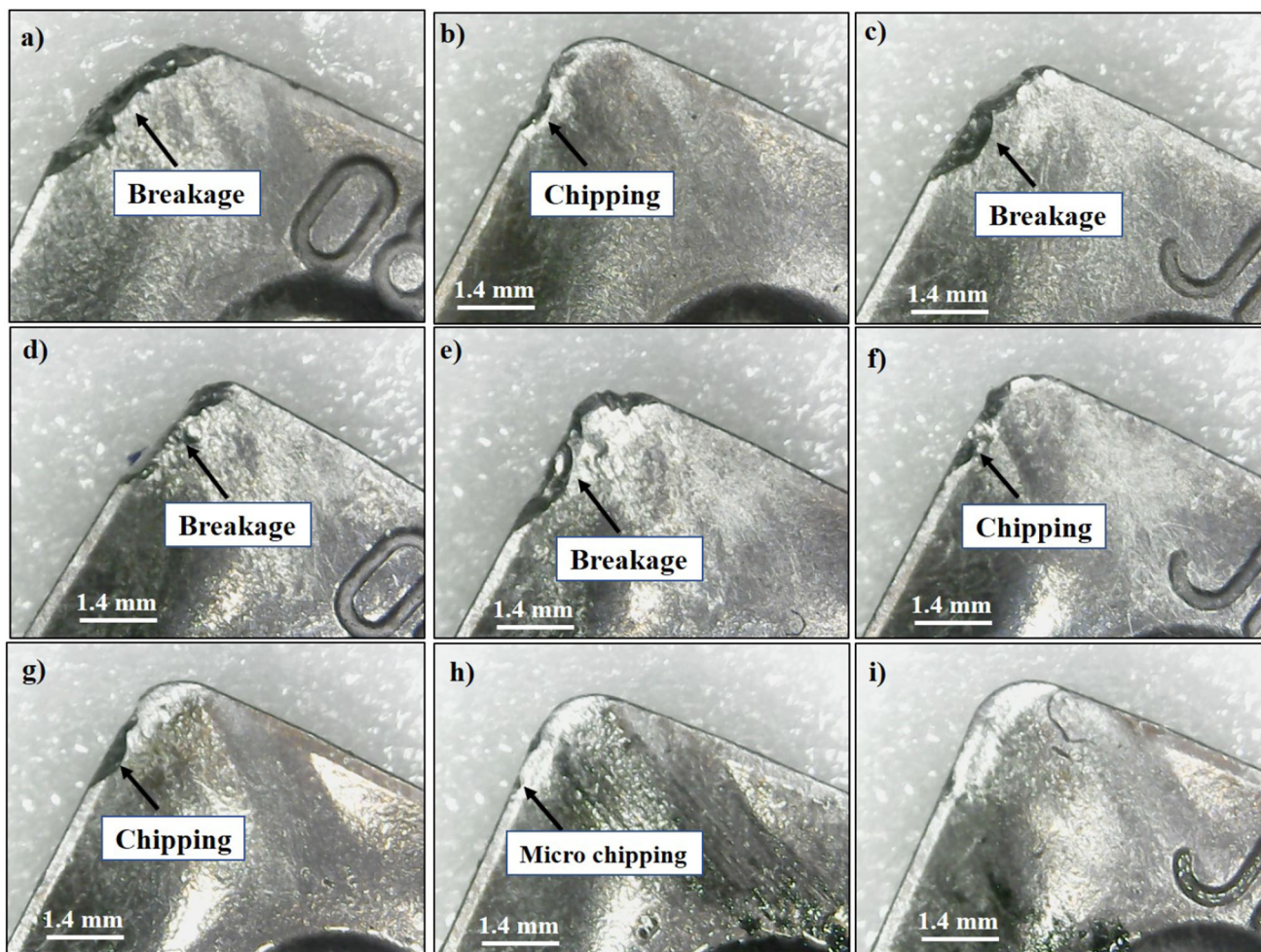
Fig. 11 Microscopic wear images of the cutting tool's rake surface (a_p = 1.5 mm), **Dry milling**: V_c = 45 m/min, f_z = 0.25 mm/tooth, **b** V_c = 60 m/min, f_z = 0.15 mm/tooth, **c** V_c = 75 m/min, f_z = 0.20 mm/tooth, **Hot milling**: **d** V_c = 45 m/min, f_z = 0.20 mm/tooth, **e** V_c = 60 m/min, f_z = 0.25 mm/tooth, **f** V_c = 75 m/min, f_z = 0.15 mm/tooth, **Hybrid milling**: **g** V_c = 45 m/min, f_z = 0.25 mm/tooth, **h** V_c = 60 m/min, f_z = 0.15 mm/tooth, **i** V_c = 75 m/min, f_z = 0.20 mm/tooth

accumulated on the cutting zone because of the lower thermal properties and lead to raising the temperature of the insert resulted in the cutting tool failure. The chipping, breakage, catastrophic failure, cracks, and plastic deformation are the common wear failures during the machining of titanium alloys [8, 40].

The highest tool failures occurred in the experiments performed in the dry milling environment at room temperature, whereas a slight reduction in tool wear happened under hot milling conditions. In hybrid machining conditions, the performance of the cutting tool improved remarkably and negligible failures were seen on the cutting tool. The severe chipping, edge breakage, and flaking wear mechanism occurred as a result of the overloading of mechanical tensile stresses depending on the cutting feed and speed rates in dry milling at room temperature and hot machining. The catastrophic failure was also formed in machining with a high cutting speed and feed rate combinations. Higher cutting feed and speed combinations caused to increase in friction at the tool and workpiece interface and generated cutting temperature in the machining zone. The workpiece exhibited adhesive behavior with the cutting tool, and therefore, chipping, edge breakage, and catastrophic failures can be attributed to the built-up edge (BUE) formation constituted on the cutting edge (Fig. 12).

The SEM micro images indicated that the adhered material on the cutting edge also caused scratches and adhered materials particles on the machined surface of the workpiece (Fig. 2). SEM analysis results have shown that BUE has an important effect on the damage mechanism of the cutting tool. In the line with the EDS results, it can be inferred that the BUE on the cutting tool was broken during the cutting process, causing chipping, edge breakage, and flaking on the insert. Figure 12 shows the wear mechanism that BUE
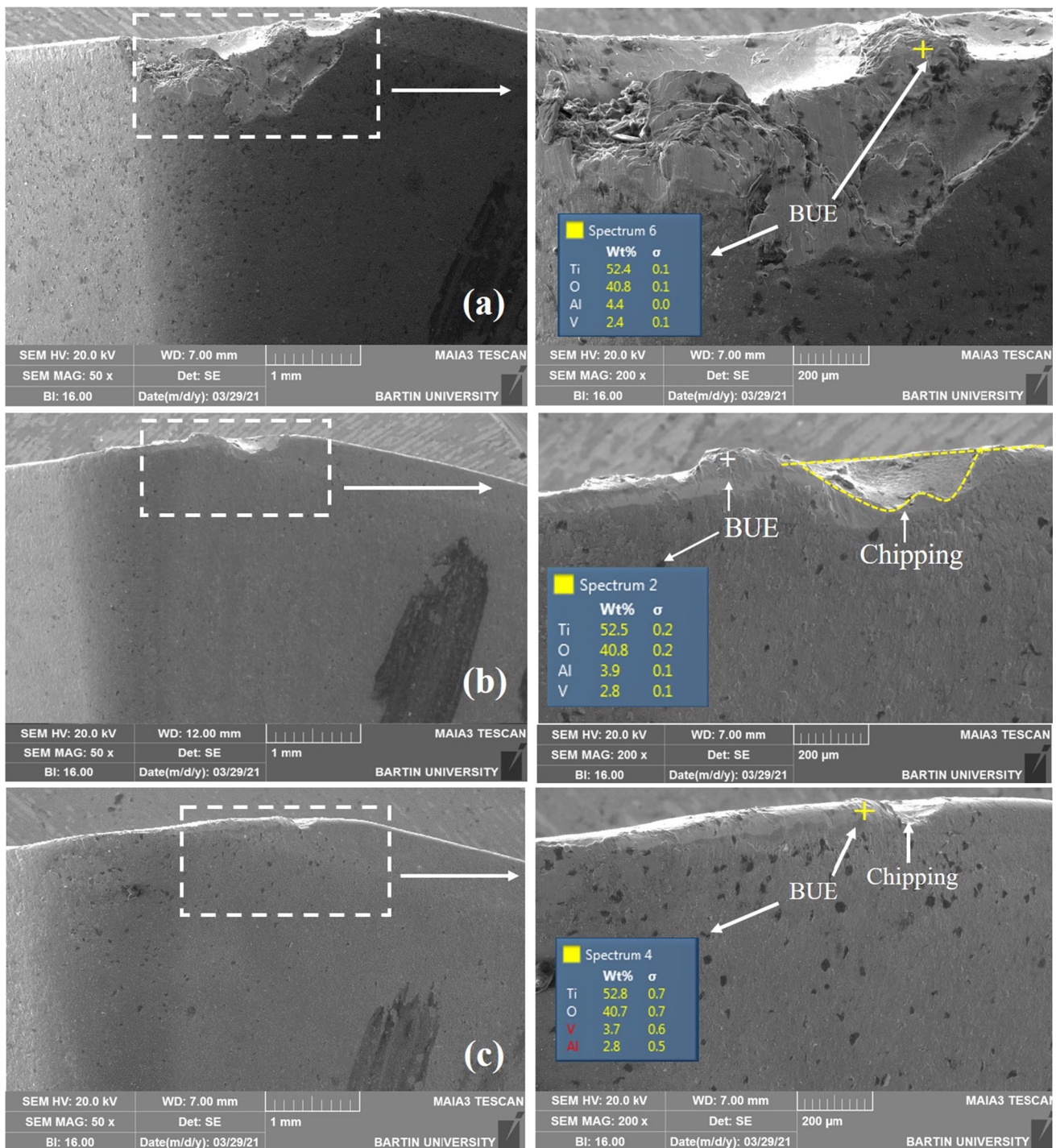
Fig. 12 SEM images of cutting insert **a** Dry milling ($V_c = 75$ m/min, $f_z = 0.25$ mm/tooth, $a_p = 1$ mm), **b** hot milling ($V_c = 75$ m/min, $f_z = 0.25$ mm/tooth, $a_p = 1$ mm) **c** hybrid milling ($V_c = 60$ m/min, $f_z = 0.20$ mm/tooth, $a_p = 1.5$ mm)

creates on the cutting tool in experiments of 3, 6, and 12 conducted at higher cutting feed and speed conditions. The chipping, and flaking mechanisms were seen in milling with low cutting feed and speed combinations according to the Taguchi experimental design. The material residues on the cutting insert were seen in milling of Ti–6Al–4V alloy both

at room temperature and hot conditions. The non-uniform wear mechanism on flank edge of the insert indicated that the cutting tool was worn by the adhering workpiece material (Fig. 12).

A small amount of chipping wear was observed on the cutting edge at cutting speeds of 45 and 60 m/min, and axial

cutting depth at 1 mm under the hybrid milling environment, whereas any wear failures were not seen at 75 m/min. Meanwhile, the cutting insert showed better performance at depth of cut of 1.5 mm under hybrid machining environments and it was found that the tool failure was decreased. The formation of BUE evidence was also observed and chip accumulation on the cutting tool's rake face under hybrid milling environments. The macro images of tool wear showed that the use of MQL during hot machining significantly improved the tool life.

It was observed that the heat generation was accumulated on the cutting zone in dry machining conditions at room temperature and the heat was decreased as it moved away from the cutting area. Hence, the cutting tool exposed heavy temperatures every feed passes to perform the plastic deformation of the workpiece. It can be concluded that generating high machining temperatures for the plastic deformation of the titanium may be a reason for quick tool wear and consequently higher power consumption and vibration.

In hot machining, the heat was distributed uniformly on the workpiece in the milling process and caused thermal softening of the titanium alloy. Therefore, the cutting tool consumed lower energy to cut the workpiece material depending on the reducing strength before reaching the cutting area resulting in decreasing wear rate, lower power consumption and vibration. The lubricant was applied to the cutting zone with pressurized air in addition of hot machining during the hybrid milling environment. The pre-heating process led to workpiece material thermal softening; MQL significantly reduced the friction along with the cooling effect on cutting tool, under the hybrid milling environment. Therefore, the improvement of tool performance can be elucidated to the reduction of temperature on the cutting edge and decreasing friction between cutting insert and chip interface when MQL used in the hybrid machining [37].

The power consumption measurements proved that the resistance of the workpiece in the milling operation performed under the hot working environment was decreased. In addition to this, the lubrication of the cutting area with the pressurized air using the MQL system reduced the friction between the chip and cutting-edge interface and provided cooling on the insert. A negligible tool wear was seen at cutting speed 45 m/min and dept of cut 1 mm, however better cutting tool performance was achieved in hybrid cutting conditions compared to other machining environments used in the experiments. Therefore, the improvement rates of tool failures can be related to the reduction of temperature on the edge of the insert and decreasing friction between cutting tool and chip interface when MQL used in the hybrid machining.

Comparison of the cutting tool wear observations at various machining parameters between dry at room temperature, and hot machining environments showed the importance of lubrication in hybrid machining on the influence of vibration, power consumption, and tool wear. SEM images and EDS results of cutting tools used in three different cutting environments under experimental study are given in Fig. 12. SEM pictures and EDS results indicated that the workpiece material adhesion (BUE) occurred on the cutting edge under all cutting environments. It was observed that the amount of adhesion rate was more in dry machining at room temperature resulting in chipping wear by causing edge fracture.

The higher material adhesion on the insert wear can be attributed to increasing contact pressure applied by the chip at lower cutting velocities [41] and insufficient heat generation during cutting. Meanwhile, it can be seen that the dimension of chipping wear on the insert decreased under the hot cutting environment. The fact that the material was heated before the chip removal process led to the formation of the heat required for cutting during the milling of titanium alloy and the cutting process to be performed more easily. Thus, less material adhesion formation occurred compared to the machining process performed at room temperature and the pre-heating process contributed to the reduction of tool failure. In the hybrid cutting environment, the pre-heated workpiece material was machined employing MQL on the rake face of the cutting insert during the milling process. The tool wear measurements, macro images, and SEM images confirmed that the lubrication/compressed air application on the cutting tool significantly reduced the wear on the insert by reducing the friction under hybrid cutting environment.

3.4 Analysis of Variance (ANOVA)

The importance levels and contribution rates of the cutting variables on power consumption, vibration, tool wear and surface roughness were evaluated by using the results of ANOVA given in Table 3.

The ANOVA outputs indicated that the cutting feed was the utmost effective machining variable with a 64% rate on surface roughness, whereas the contribution of the cutting environment was 23%. The axial cutting depth and cutting speed did not indicate significant effect on surface roughness and calculated the contribution rate as 5% and 3%, respectively.

The cutting environment was the most significant cutting variable with percentage contribution of 75% in controlling the vibration of machine tool. The contribution of the cutting feed, cutting speed and axial cutting depth were computed as 9%, 8% and 2%, respectively. Similarly, the ANOVA results showed that the primary significant cutting variables for the power consumption were cutting feed (36%) [41] and cutting environment (33%) were followed by axial cutting depth (20%) and cutting speed (4%). For tool wear, it was seen that the most effective milling parameter were determined to be cutting environment with an accumulated contribution of

Table 3 Results of the analysis of variance for output variables

Source	DF	Adj SS	Adj MS	F-value	P-value	Contribution rate (%)
Surface roughness, (Ra)						
C_e	1	0.031416	0.031416	57.55	0.000	23%
V_c	1	0.004135	0.004135	7.57	0.016	3%
f_z	1	0.087253	0.087253	159.84	0.000	64%
a_p	1	0.007442	0.007442	13.63	0.003	5%
Error	13	0.007096	0.000546			5%
Total	17	0.137343				100%
Vibration, (V)						
C_e	1	0.57787	0.577870	176.32	0.000	75%
V_c	1	0.06068	0.060681	18.52	0.001	8%
f_z	1	0.06700	0.067001	20.44	0.001	9%
a_p	1	0.01784	0.017840	5.44	0.036	2%
Error	13	0.04261	0.003277			6%
Total	17	0.766				100%
Power consumption, (P)						
C_e	1	1,044,890	1,044,890	52.87	0.000	33%
V_c	1	116,230	116,230	5.88	0.031	4%
f_z	1	1,138,368	1,138,368	57.6	0.000	36%
a_p	1	636,568	636,568	32.21	0.000	20%
Error	13	256,922	19,763			8%
Total	17	3,192,979				100%
Tool wear, (VB)						
C_e	1	0.248544	0.248544	53.73	0.000	48%
V_c	1	0.008911	0.008911	1.93	0.188	2%
f_z	1	0.199950	0.199950	43.23	0.000	39%
a_p	1	0.000235	0.000235	0.05	0.825	0%
Error	13	0.060134	0.004626			12%
Total	17	0.517774				100%

48%. The contribution of the cutting feed, cutting speed and axial cutting depth were as 39%, 2% and 0%, respectively.

The optimal milling variables were defined using the response table for S/N ratios given in Table 4. As mentioned previously, higher *S/N* ratios identifies the lowest values of the surface roughness, vibration, power consumption, and cutting tool wear. Therefore, the highest S/N ratios marked as bold in Table 4, indicate the favorable milling parameters. The optimal surface roughness values were achieved at cutting environment of level 1 (*S/N* = 3.559) at cutting speed of level 3 (*S/N* = 3.075), at feed rate of level 1 (*S/N* = 3.906), and at axial cutting depth of level 1 (*S/N* = 3.106). The *S/N* ratio results given in Table 4 showed that the hybrid machining has the highest S/N ratio compared with the machining at room temperature and hot machining environments for vibration and power consumption. It can be noted that the favorable values for vibration were obtained at cutting environment of level 3 (*S/N* = 7.438), at cutting speed of level

1 (*S/N* = 5.088), at feed rate of level 1 (*S/N* = 5.47), and at axial cutting depth of level 1 (*S/N* = 4.93). The minimum energy consumption was achieved at cutting environment of level 3 (*S/N* = −59.04), at cutting speed of level 3 (*S/N* = −60.62), at feed rate of level 1 (*S/N* = −59.02), and at axial cutting depth of level 1 (*S/N* = −59.99). Similarly, the minimum tool wear values were measured at cutting environment of level 3 (*S/N* = 30.30), at cutting speed of level 3 (*S/N* = 22.78), at feed rate of level 1 (*S/N* = 28.70), and at axial cutting depth of level 1 (*S/N* = 20.33). The analysis revealed that the highest cutting speed (75 m/min), the lowest cutting feed (0.15 mm/tooth) and axial cutting depth (1 mm) should be used for the quality of surface in machining of titanium at room temperature. However, it was observed that there was a 0.1 µm improvement on surface quality as compared to hot and hybrid milling conditions. Hence, it can be said

Table 4 The S/N ratios for *Ra*, *V*, *P* and VB (Smaller is better, optimal machining variables and the best level of each control factor are indicated in bold)

Level	*Ce*	*V*$_c$	*f*$_z$	*a*$_p$
Surface roughness (Ra)				
1	**3.559**	2.699	**3.906**	**3.106**
2	2.699	2.819	2.824	2.622
3	2.334	**3.075**	1.863	
Delta	1.225	0.376	2.043	0.485
Rank	2	4	1	3
Vibration (V)				
1	1.374	**5.088**	**5.47**	**4.93**
2	4.406	4.707	4.172	3.882
3	**7.438**	3.424	3.577	
Delta	6.064	1.664	1.893	1.048
Rank	1	3	2	4
Power consumption (P)				
1	− 63.33	− 62.12	**− 59.02**	**− 59.99**
2	− 61.44	− 61.07	− 61.4	− 62.55
3	**− 59.04**	**− 60.62**	− 63.4	
Delta	4.3	1.51	4.38	2.55
Rank	2	4	1	3
Tool wear, (VB)				
1	10.27	18.08	**28.70**	**20.33**
2	17.70	17.41	18.22	18.52
3	**30.30**	**22.78**	11.35	
Delta	20.03	5.37	17.35	1.80
Rank	1	3	2	4

that hybrid milling should be recommended for the minimum vibration, power consumption and better cutting-edge performance in machining of Ti–6Al–4V alloy.

3.5 Microstructure

The microstructure images of the machined surface of workpiece under various cutting environments used in the experiments are shown in Fig. 13. Titanium alloys maintain their chemical and physical properties at high cutting temperatures. However, with the aim to preserve the superior mechanical properties and microstructural stability of the titanium alloy, it is necessary to pay attention to the strain hardening, thermal softening, and grain refinement on the processed surface.

At high temperatures, the size of the grains on the machined surface of the workpiece rises with the effect of heat, whereas the mechanical properties and hardness decrease. At the same time, the grain boundary sliding may occur on the machined surface at high temperatures and this

may cause gaps in the line of the grain boundaries. Then, the force applied by the cutting tool on the workpiece surface during the machining process can distort the grains. Meanwhile, if the workpiece material subjected to rapid cooling during the machining process, the size of the grains decreases resulting in grain refinements and an increase in the surface hardness of the workpiece occurs. As a result, the cutting environment used during chip removal from the material should not has a negative influence on the mechanical properties of the material. When the grain structures formed on the surface of the material are examined, it can be seen that the microstructures obtained in hot working and hybrid cutting environments have the same properties as the machined at room temperature. In addition, the microhardness measurements were performed on the surface and subsurface of the machined part to see the effect of the heating process.

Figure 14 shows the microhardness values taken at 1 mm intervals from the machined surface and machined subsurface. The mean microhardness values of the machined surface under dry at room temperature (Test 3), hot milling (Test 6), hybrid milling (Test 18), and confirmation test in hybrid milling (C5, at cutting speed 45 m/min, at feed rate 0.15 mm/rev, and at depth of cut 1 mm) were 324 HV, 311 HV, 312 HV, and 303 HV, respectively. The highest microhardness was obtained in T3 performed under the dry environment at room temperature. The pre-heating process caused a reduction of 4% in microhardness value compared to under dry environment at room temperature on the machined surface due to increasing grain size with the effect of the heating operation. Meanwhile, it was found that the microhardness values of machined subsurface under hot and hybrid milling environments were higher than the machined surface. Consequently, it may be concluded that the machined surface was affected pre-heating process resulting in a small amount of reduction in microhardness. According to the optical images and microhardness values, it can be seen that the preheating process applied to the material did not indicate a negative effect on the grain size and microhardness of the machined surface of titanium alloy. These results could be attributed that the layer of material exposed to heat was removed with the chip during the milling process.

4 Conclusions

In this study, Ti–6Al–4V alloy was subjected to the face milling experiments based on a Taguchi L18 orthogonal array involved dry at room temperature, hot, and hybrid cutting environments. A pre-heating process was applied to the workpiece material under hot and hybrid cutting environments. In addition to the pre-heating process, an MQL was employed to the rake surface of the insert under hybrid cutting environment experiments of Ti–6Al–4V. The effects of
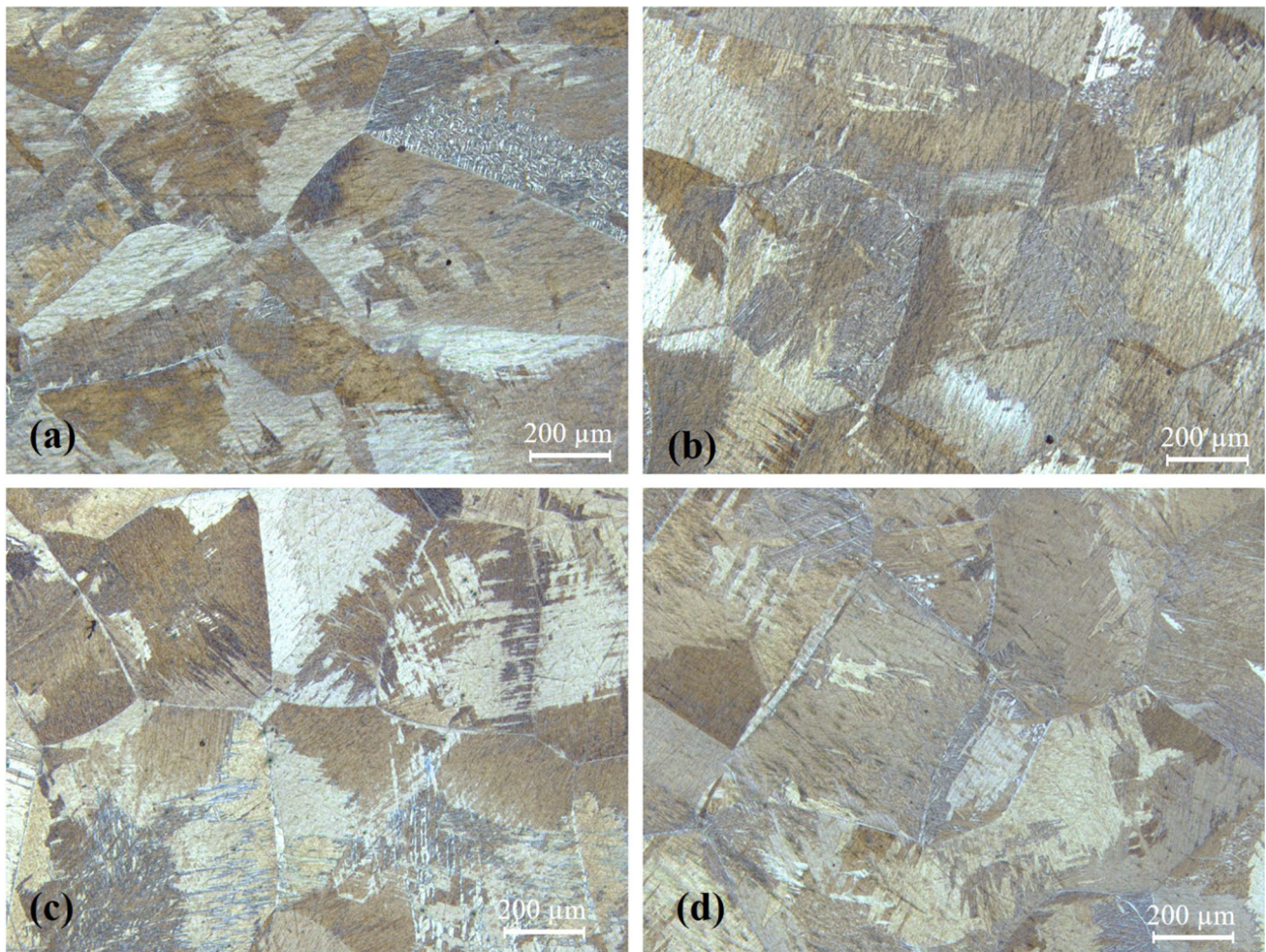
Fig. 13 Optical images of machined surface, **a** Dry milling ($V_c = 75$ m/min, $f_z = 0.25$ mm/tooth, $a_p = 1$ mm), **b** hot milling ($V_c = 75$ m/min, $f_z = 0.25$ mm/tooth, $a_p = 1$ mm), **c** hybrid milling ($V_c = 60$ m/min, $f_z = 0.20$ mm/tooth, $a_p = 1.5$ mm), and **d** hybrid milling ($V_c = 45$ m/min, $f_z = 0.15$ mm/rev, $a_p = 1$ mm)

Fig. 14 Mean microhardness values of the surface and subsurface of machined surface under study
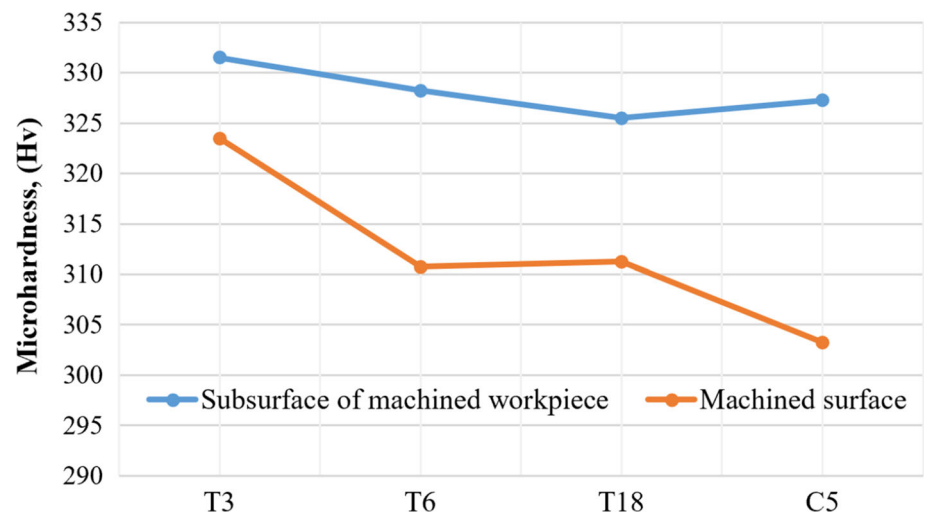
the pre-heating process and cooling-lubrication approach in hot machining were studied on the tool wear, surface roughness, power consumption, and vibration. The experimental results are summarized as follows:

- Better surface roughness values were achieved in milling at room temperature. It was seen that the material smearing occurred on the machined surface of the workpiece, resulting in a 15% increase in surface roughness values in the hot and hybrid milling. The feed rate was the most effective cutting variable on surface roughness with a contribution of 64%, followed by the cutting environments with a contribution of 23%.

- The machine tool vibration and power consumption decreased by a 106% and 64% rate in milling of hot and hybrid environments compared to the dry milling. The effects of the cutting environment on the vibration, and power consumption were 75%, and 33%, respectively.

- The lowest average tool wear was calculated as 0.06 mm in hybrid milling, whereas the highest mean tool wear was 0.35 mm in dry milling. The severe chipping and catastrophic failure were seen on the cutting edge in milling at room temperature and hot milling environment. A better cutting tool performance was obtained in the hybrid milling environment.

- The optimal surface roughness values were observed at $A_1B_3C_1D_1$ i.e., cutting environment at room temperature, cutting speed at 75 m/min, feed rate at 0.15 mm/tooth, and axial cutting depth at 1 mm, respectively. The minimum energy consumption and cutting tool wear were achieved at $A_3B_3C_1D_1$ ci.e., cutting environment at hybrid, cutting speed at 75 m/min, feed rate at 0.15 mm/tooth, and axial cutting depth at 1 mm. Similarly, the minimum machine tool vibration was recorded at $A_3B_1C_1D_1$ i.e., cutting environment at hybrid, cutting speed at 40 m/min, feed rate at 0.15 mm/tooth, and axial cutting depth at 1 mm.

- The grain sizes on the machined surfaces of the specimens were not affected by the heating, and a reduction of 4% in microhardness on the machined surface was measured over the milling at room temperature.

References

1. Shokrani, A.; Al-Samarrai, I.; Newman, S.T.: Hybrid cryogenic MQL for improving tool life in machining of Ti–6Al–4V titanium alloy. J. Manuf. Process. **43**, 229–243 (2019). https://doi.org/10.1016/j.jmapro.2019.05.006

2. Nath, C.; Kapoor, S.G.; Srivastava, A.K.: Finish turning of Ti–6Al–4V with the atomization-based cutting fluid (ACF) spray system. J. Manuf. Process. **28**, 464–471 (2017). https://doi.org/10.1016/j.jmapro.2017.04.013

3. Hoyne, A.C.; Nath, C.; Kapoor, S.G.: On cutting temperature measurement during titanium machining with an atomization-based cutting fluid spray system. J. Manuf. Sci. Eng. Trans. ASME. **137**, 1–7 (2015). https://doi.org/10.1115/1.4028898

4. Shokrani, A.; Dhokia, V.; Newman, S.T.: Investigation of the effects of cryogenic machining on surface integrity in CNC end milling of Ti–6Al–4V titanium alloy. J. Manuf. Process. **21**, 172–179 (2016). https://doi.org/10.1016/j.jmapro.2015.12.002

5. Shokrani, A.; Dhokia, V.; Newman, S.T.: Comparative investigation on using cryogenic machining in CNC milling of Ti–6Al–4V titanium alloy. Mach. Sci. Technol. **20**, 475–494 (2016). https://doi.org/10.1080/10910344.2016.1191953

6. Pandey, K.; Datta, S.: Materials today: proceedings hot machining of difficult-to-cut materials: a review. Mater. Today Proc. (2021). https://doi.org/10.1016/j.matpr.2020.12.687

7. AbdulkareemMohammed, K.; Abdulhameed, J.J.; Al-Ameen, E.S.: The effectiveness of hot machining process for the machinability of hard to cut materials: a review. IOP Conf. Ser. Mater. Sci. Eng. (2020). https://doi.org/10.1088/1757-899X/870/1/012140

8. Agrawal, C.; Wadhwa, J.; Pitroda, A.; Pruncu, C.I.; Sarikaya, M.; Khanna, N.: Comprehensive analysis of tool wear, tool life, surface roughness, costing and carbon emissions in turning Ti–6Al–4V titanium alloy: cryogenic versus wet machining. Tribol. Int. **153**, 106597 (2021). https://doi.org/10.1016/j.triboint.2020.106597

9. Ha, J.H.; Lee, C.M.: A study on the thermal effect by multi heat sources and machining characteristics of laser and induction assisted milling. Mater. (Basel). (2019). https://doi.org/10.3390/ma12071032

10. Ginta, T.L.; Amin, A.K.M.N.: Thermally-assisted end milling of titanium alloy Ti–6Al–4V using induction heating. Int. J. Mach. Mach. Mater. **14**, 194–212 (2013). https://doi.org/10.1504/IJMMM.2013.055737

11. Upadhyay, V.; Jain, P.K.; Mehta, N.K.: Machinability studies in hot machining of Ti–6Al–4V alloy. AMR **622–623**, 361–365 (2012)

12. Kumar, A.K.; Venkataramaiah, P.: Heat assisted machining of inconel 718 Alloy using abaqus/explicit. Mater. Today Proc. **18**, 4531–4536 (2019). https://doi.org/10.1016/j.matpr.2019.07.424

13. Madhavulu, G.; Ahmed, B.: Hot machining process for improved metal removal rates in turning operations. J. Mater. Process. Technol. **44**, 199–206 (1994)

14. Leshock, C.E.; Kim, J.N.; Shin, Y.C.: Plasma enhanced machining of Inconel 718: Modeling of workpiece temperature with plasma heating and experimental results. Int. J. Mach. Tools Manuf. **41**, 877–897 (2001). https://doi.org/10.1016/S0890-6955(00)00106-1

15. Wang, Z.Y.; Rajurkar, K.P.; Fan, J.; Lei, S.; Shin, Y.C.; Petrescu, G.: Hybrid machining of Inconel 718. Int. J. Mach. Tools Manuf. **43**, 1391–1396 (2003). https://doi.org/10.1016/S0890-6955(03)00134-2

16. López De Lacalle, L.N.; Sánchez, J.A.; Lamikiz, A.; Celaya, A.: Plasma assisted milling of heat-resistant superalloys. J. Manuf. Sci. Eng. Trans. ASME. **126**, 274–285 (2004). https://doi.org/10.1115/1.1644548

17. Cao, X.F.; Woo, W.S.; Lee, C.M.: A study on the laser-assisted milling of 13–8 stainless steel for optimal machining. Opt. Laser Technol. **132**, 106473 (2020). https://doi.org/10.1016/j.optlastec.2020.106473

18. Amin, A.K.M.N.; Abdelgadir, M.: The effect of preheating of work material on chatter during end milling of medium carbon steel performed on a vertical machining center (VMC). J. Manuf. Sci. Eng. Trans. ASME. **125**, 674–680 (2003). https://doi.org/10.1115/1.1596557

19. Brecher, C.; Emonts, M.; Rosen, C.J.; Hermani, J.P.: Laser-assisted milling of advanced materials. Phys. Proc. **12**, 599–606 (2011). https://doi.org/10.1016/j.phpro.2011.03.076

20. Hossain, M.I.; Amin, A.K.M.N.; Patwari, A.U.; Karim, A.: Enhancement of machinability by workpiece preheating in end milling of Ti–6Al–4V. **31**, 320–326 (2008)

21. Ginta, T.L.; Amin, A.K.M.N.; Lajis, M.A.; Karim, A.N.M.; Radzi, H.C.D.M.: Improved tool life in end milling Ti–6Al–4V through workpiece preheating. Eur. J. Sci. Res. **27**, 384–391 (2009)

22. Kim, E.J.; Lee, C.M.: A study on the optimal machining parameters of the induction assisted milling with Inconel 718. Mater. (Basel). (2019). https://doi.org/10.3390/ma12020233

23. Kim, E.J.; Lee, C.M.: Experimental study on power consumption of laser and induction assisted machining with inconel 718. J. Manuf. Process. **59**, 411–420 (2020). https://doi.org/10.1016/j.jmapro.2020.09.064

24. Maity, K.P.; Swain, P.K.: An experimental investigation of hot-machining to predict tool life. J. Mater. Process. Technol. **198**, 344–349 (2008). https://doi.org/10.1016/j.jmatprotec.2007.07.018

25. Venkatesh, G.; Chakradhar, D.: Influence of thermally assisted machining parameters on the machinability of inconel 718 superalloy. SILICON **9**, 867–877 (2017). https://doi.org/10.1007/s12633-017-9568-3

26. Parida, A.K.; Maity, K.: Study of machinability in heat-assisted machining of nickel-base alloy. Meas. J. Int. Meas. Confed. **170**, 108682 (2021). https://doi.org/10.1016/j.measurement.2020.108682

27. Parida, A.K.; Maity, K.: Hot machining of Ti–6Al–4V: FE analysis and experimental validation. Sadhana Acad. Proc. Eng. Sci. **44**, 1–6 (2019). https://doi.org/10.1007/s12046-019-1127-8

28. Parida, A.K.; Maity, K.: Experimental investigation on tool life and chip morphology in hot machining of Monel-400. Eng. Sci. Technol. Int. J. **21**, 371–379 (2018). https://doi.org/10.1016/j.jestch.2018.04.003

29. Alkali, A.U.; Ginta, T.L.; Abdulrani, A.M.; Fawad, H.; Danish, M.: Study on the machinability of 316L stainless steel using flame assisted machining. ARPN J. Eng. Appl. Sci. **11**, 8743–8749 (2016)

30. Amin, A.; Talantov, N.V.: Influence of the instability of chip formation and preheating of work on tool life in machining high temperature resistant steel and titanium alloys (1986)

31. Li, C.; Xu, M.; Yu, Z.; Huang, L.; Li, S.; Li, P.; Niu, Q.; Ko, T.J.: Electrical discharge-assisted milling for machining titanium alloy. J. Mater. Process. Technol. **285**, 116785 (2020). https://doi.org/10.1016/j.jmatprotec.2020.116785

32. Liu, Y.; Geng, D.; Shao, Z.; Zhou, Z.; Jiang, X.; Zhang, D.: A study on strengthening and machining integrated ultrasonic peening drilling of Ti–6Al–4V. Mater. Des. **212**, 110238 (2021). https://doi.org/10.1016/j.matdes.2021.110238

33. Mruthunjaya, M.; Yogesha, K.B.: A review on conventional and thermal assisted machining of titanium based alloy. Mater. Today Proc. (2021). https://doi.org/10.1016/j.matpr.2021.03.490

34. Pimenov, D.Y.; Mia, M.; Gupta, M.K.; Machado, A.R.; Tomaz, Í.V.; Sarikaya, M.; Wojciechowski, S.; Mikolajczyk, T.; Kaplonek, W.: Improvement of machinability of Ti and its alloys using cooling-lubrication techniques: a review and future prospect. J. Mater. Res. Technol. **11**, 719–753 (2021). https://doi.org/10.1016/j.jmrt.2021.01.031

35. Sarıkaya, M.; Gupta, M.K.; Tomaz, I.; Pimenov, D.Y.; Kuntoğlu, M.; Khanna, N.; Yıldırım, Ç.V.; Krolczyk, G.M.: A state-of-the-art review on tool wear and surface integrity characteristics in machining of superalloys. CIRP J. Manuf. Sci. Technol. **35**, 624–658 (2021). https://doi.org/10.1016/j.cirpj.2021.08.005

36. ISO/TS 80004-2:2015: ISO 8688-1:1989 Tool life testing in milling—Part 1: Face milling. 2018, 27000 (2019)

37. Moghadasi, A.; Hadad, M.: Towards sustainable machining of 17–4 PH stainless steel using hybrid MQL-hot turning process. Energy Equip. Syst. **7**(4), 339–352 (2019)

38. Sen, B.; Gupta, M.K.; Mia, M.; Pimenov, D.Y.; Mikolajczyk, T.: Performance assessment of minimum quantity castor-palm oil mixtures in hard-milling operation. Mater. (Basel) **14**, 1–13 (2021). https://doi.org/10.3390/ma14010198

39. Salur, E.; Kuntoğlu, M.; Aslan, A.; Pimenov, D.Y.: The effects of MQL and dry environments on tool wear, cutting temperature, and power consumption during end milling of AISI 1040 steel. Metals **11**(11), 1674 (2021)

40. Sun, S.; Brandt, M.; Mo, J.P.T.: Evolution of tool wear and its effect on cutting forces during dry machining of Ti–6Al–4V alloy. Proc. Inst. Mech. Eng. B J. Eng. Manuf. **228**, 191–202 (2014). https://doi.org/10.1177/0954405413500243

41. Mane, S.; Joshi, S.S.; Karagadde, S.; Kapoor, S.G.: Modeling of variable friction and heat partition ratio at the chip-tool interface during orthogonal cutting of Ti–6Al–4V. J. Manuf. Process. **55**, 254–267 (2020). https://doi.org/10.1016/j.jmapro.2020.03.035